Eur. Phys. J. B **6**, 277–292 (1998)

THE EUROPEAN PHYSICAL JOURNAL B

Modeling film flows down inclined planes

C. Ruyer-Quil[a] and P. Manneville[b]

Laboratoire d'Hydrodynamique[c], École Polytechnique, 91128 Palaiseau, France

Received: 16 April 1998 / Revised: 29 June 1998 / Accepted: 2 July 1998

Abstract. A new model of film flow down an inclined plane is derived by a method combining results of the classical long wavelength expansion to a weighted-residuals technique. It can be expressed as a set of three coupled evolution equations for three slowly varying fields, the thickness h, the flow-rate q, and a new variable τ that measures the departure of the wall shear from the shear predicted by a parabolic velocity profile. Results of a preliminary study are in good agreement with theoretical asymptotic properties close to the instability threshold, laboratory experiments beyond threshold and numerical simulations of the full Navier–Stokes equations.

PACS. 47.20M Interfacial instability – 47.20K Nonlinearity

1 Introduction

In addition to being involved in a wide variety of technical applications (chemical reactors, evaporators, *etc.*), the dynamics of fluid films is an interesting topic in itself. As a matter of fact, thin films flowing down inclined surfaces exhibit a rich phenomenology [1] and offer a good testing ground for the study of the transition to turbulence. Instabilities take place at low flow rates, which gives a unique opportunity to analyze the development of waves at the surface of the fluid into large-amplitude strongly nonlinear localized structures such as solitary pulses and further to study their disorganization into developed spatio-temporal chaos *via* secondary instabilities.

A trivial solution to the flow equations is easily found in the form of a steady uniform parallel flow with parabolic velocity profile, often called Nusselt's solution, where the work done by gravity is exactly consumed by viscous dissipation. Thin films at low flow rate over sufficiently steep surfaces turn out to be unstable against long wavelength infinitesimal perturbations, *i.e.* wavelength large when compared to the thickness of the flow. This is confirmed by a general study of the relevant Orr–Sommerfeld equation which shows that short-wavelength shear instabilities of the Tollmien–Schlichting type are only relevant for flows over planes at vanishingly small inclination angles and very high flow rates [2].

In the following we will thus be concerned with long wavelength interfacial instability modes, the dynamics of which is essentially controlled by viscosity and surface tension effects. Close to the threshold these waves present themselves as stream-wise surface undulations free of span-wise modulations ("two-dimensional" waves) emerging from a supercritical (*i.e.*, continuous) bifurcation. Farther from threshold, they saturate at finite amplitudes and, depending on control parameters, may develop secondary instabilities involving span-wise modulations ("three-dimensional" instabilities) [3] or first evolve into localized "solitary" structures that subsequently destabilize [4]. For the moment we will focus on the two-dimensional case where the hydrodynamic fields depend only on the cross-stream and stream-wise coordinates, y and x respectively (see Fig. 1), leaving the three-dimensional problem for future study.

It turns out that, for the regimes we are interested in, the height of the waves remains small when compared to their wavelength. This motivates a long standing practice [5,6] of studying them by means of asymptotic expansions in powers of a small parameter ϵ, usually called the *film parameter*. Starting from this long-wave expansion, a certain number of models have then been derived since the pioneering work of Kapitza [7], *e.g.* [8–10] for the most recent ones, see the review by Demekhin *et al.* [11] for earlier attempts. The simplest useful result obtained in this way is a partial differential equation called Benney's equation [12] to be written explicitly later (36). Governing the local thickness of the film $h(x,t)$ in terms of its space-time derivatives, it will be written here simply as $\partial_t h = G(h^n, \partial_{x^m} h)$, where G involves various algebraic powers and differentiation orders (n,m) of h. Within this approach the film evolution is modeled in terms of lubrication theory, which results in the enslaving of flow variables to the local film height, *i.e.* a reduction to some *effective dynamics* for the interface through the elimination of degrees of freedom associated to velocity field.

[a] e-mail: `ruyer@ladhyx.polytechnique.fr`
[b] e-mail: `pops@ladhyx.polytechnique.fr`
[c] CNRS UMR n° 7646.

The simplification brought by this reduction has mainly permitted a first study of the nonlinear development of waves using the tools of dynamical systems theory [13], study that was continued using the celebrated Kuramoto–Sivashinsky (KS) equation [14], obtained in the present context by taking the limit of small amplitude modulations [15,16]. By contrast with the KS equation, Benney's equation can lead to a non-physical evolution with the development of finite-time singularities [13,17]. Such an evolution strongly limits its use to a narrow neighborhood of the threshold where the KS equation —that does not behave so wildly— is expected to give already valuable results.

Numerical investigation of the full Navier-Stokes (NS) equations, though conceivable, is cumbersome owing to the presence of a free boundary. Though it can (should) serve as a check point for models in the two-dimensional case, the only one to be reliably implemented up to now [18,19], the numerical approach does not give much insight into the mechanisms of chaotic wave motion and pattern formation. An intermediate level of modeling is obtained in terms of so-called *boundary layers equations* (BL) [20], *i.e.* reduced NS equations incorporating the condition that stream-wise gradients are small when compared to cross-stream variations. Though one is left with a problem that has the same dimensionality as the original one, it is a little simpler and leads to lighter computations giving realistic results [21].

A subsequent level of modeling is achieved by assuming a specific shape for the velocity profile and averaging the stream-wise momentum equation in order to relate the thickness h of the film to the local flow rate $q = \int_0^h u(y)\,dy$. The first such *integral boundary layer model* was derived by Shkadov [22]. We will reobtain it below as system (49, 50). The assumption about the velocity profile and the averaging procedure are in fact two specific ingredients of a more general method for solving the BL equations in terms of *weighted residuals* [23] instead of standard discrete methods (*e.g.*, finite differences). The limitations of Shkadov's model come from the lack of freedom in the description of the hydrodynamic fields and the too rustic character of the consistency condition expressed *via* the averaging. In spite of these limitations, problems that could only be approached through black-box numerical computations of full or reduced NS equations can now be dealt with a set of partial differential equations with reduced space dimensionality (1 instead of 2). Accordingly, properties of nonlinear waves can again be studied in their rest-frame using the tools of dynamical systems theory [24, 25]. Better approximations of the flow have to be developed in order to get more realistic results. This requisite has lead to the derivation of improved models by weighted residual methods [9,10], by expanding the hydrodynamic fields on a functional basis of the cross-stream variable y, finding relations between the coefficients of the (truncated) expansion from the NS or BL equations by some specific projection rule, and further applying the resulting set of equations to concrete problems such as the structure of solitary waves. In the absence of clear physical meaning for the coefficients appearing in the expansion, the interpretation of such studies is not straightforward and one is often confined to a comparison of the obtained output with that of concurrent models and numerical solutions of BL or NS equations, or with the results of laboratory experiments.

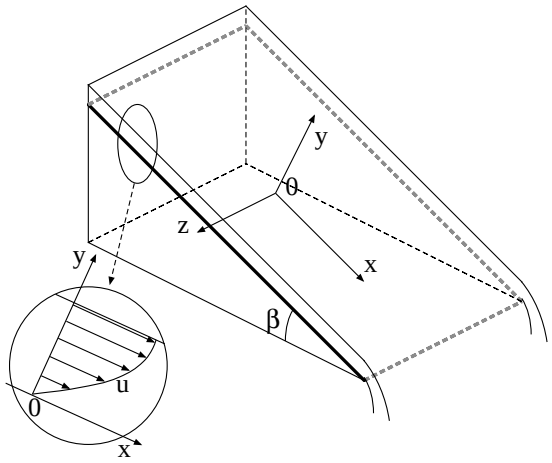

Fig. 1. Fluid film flowing down an inclined plane: definition of the geometry.

In this paper, after having recalled the governing equations (Sect. 2) of the two-dimensional problem to which we will restrict, we briefly repeat the first steps of the Benney's gradient expansion for the dynamics of film flows (Sect. 3) that will be useful to us afterward. We then develop our model in two steps, mostly for pedagogical reasons (Sects. 4 and 5). We follow the same general strategy as Yu *et al.* [9] and use BL equations as a starting point, which has the interest of focusing on the appropriate long wavelength properties of the flow right from the beginning. We also use polynomials to expand the velocity field but, to stay closer to the physics of the problem, instead of choosing some general systematic expressions of increasing degree, we prefer to take the specific polynomials that appear in Benney's gradient expansion and to introduce combinations of coefficients of the lowest order terms that may be given an immediate physical interpretation. The first-order problem (Sect. 4) involves two polynomials, the zeroth-order parabolic profile and a correction issued from Benney's expansion. Relevant coefficients involve the flow rate q, and a new field called τ measuring the departure of the wall shear from the shear predicted by a parabolic velocity profile. At this order, τ is slaved to h and q and can be eliminated adiabatically, yielding a set of two partial differential equations (9, 58) with the same structure as Shkadov's model but different coefficients. With respect to the latter, the advantage of our first-order model is to give a more accurate description of the vicinity of the instability threshold, and in particular to predict the critical flow rate exactly. At second order (Sect. 5), τ becomes a degree of freedom for its own and four well-chosen supplementary polynomials are introduced, the coefficients of which can be eliminated to yield a system of three equations (78–80) governing h, q, and τ. Sections 6 and 7 are devoted

to a discussion of our achievements focusing on a qualitative comparison of experimental and numerical results in the linear and nonlinear regimes, with preliminary numerical simulations of (78–80) and on the physical understanding that can be expected from our model.

2 Governing equations

The geometry is defined in Figure 1: the inclined plane makes an angle β with the horizontal. As usual, $\hat{\mathbf{x}}$, $\hat{\mathbf{y}}$, and $\hat{\mathbf{z}}$ are unit vectors in the stream-wise, cross-stream, and span-wise directions respectively. Here we only consider the two-dimensional case where the solution is independent of coordinate z, the extension to the full three-dimensional case does not present conceptual difficulties.

The basic (2D) equations read

$$\rho\left[\partial_t u + u\,\partial_x u + v\,\partial_y u\right] = -\partial_x p + \rho g \sin\beta + \mu\left(\partial_{xx}+\partial_{yy}\right) u, \tag{1}$$

$$\rho\left[\partial_t v + u\,\partial_x v + v\,\partial_y v\right] = -\partial_y p - \rho g \cos\beta + \mu\left(\partial_{xx}+\partial_{yy}\right) v, \tag{2}$$

$$\partial_x u + \partial_y v = 0, \tag{3}$$

where u and v denote x and y velocity components, and p the pressure. ρ is the density, μ the viscosity, and g the intensity of the gravitational acceleration.

These equations must be completed with boundary conditions at $y = 0$ or $y = h$. They will be denoted as $w\big|_0$ or $w\big|_h$ where $w(x, y, t)$ is a generic name for the pressure field, the velocity components and their derivatives. The first such condition:

$$\partial_t h + u\big|_h\,\partial_x h = v\big|_h, \tag{4}$$

simply expresses the fact that the interface $h(x, t)$ is a material line. The continuity of the stress at $y = h$ adds two more equations. The normal component reads

$$\frac{\gamma\,\partial_{xx} h}{\left[1+(\partial_x h)^2\right]^{3/2}} + \frac{2\mu}{1+(\partial_x h)^2}\left[\partial_x h\left(\partial_y u\big|_h + \partial_x v\big|_h\right) - (\partial_x h)^2\,\partial_x u\big|_h - \partial_y v\big|_h\right] + p\big|_h - p_a \;=\; 0 \tag{5}$$

where coefficient γ is the surface tension and the term in $\partial_{xx} h$ describes the curvature of the interface (p_a is the atmospheric pressure). For the tangential component one gets

$$0 = 2\partial_x h\left(\partial_y v\big|_h - \partial_x u\big|_h\right) + \left[1-(\partial_x h)^2\right]\left(\partial_y u\big|_h + \partial_x v\big|_h\right). \tag{6}$$

Finally, the no-slip condition at the rigid bottom, $y = 0$, reads:

$$u\big|_0 = v\big|_0 = 0. \tag{7}$$

It will turn interesting to replace the kinematic condition (4) at $y = h$ by an equivalent equation derived from the continuity condition. Integrating (3) over the interval $[0, h]$ we obtain:

$$0 = \int_0^h (\partial_x u + \partial_y v)\,dy = \int_0^h \partial_x u\,dy + v\big|_h - v\big|_0 = \partial_t h + \left[u\big|_h \partial_x h + \int_0^h \partial_x u\,dy\right] = \partial_t h + \partial_x \int_0^h u\,dy$$

using $v\big|_h$ given by (4) and $v\big|_0 = 0$ from (7). Defining the local instantaneous flow rate as

$$q(x,t) = \int_0^{h(x,t)} u(x, y, t)dy, \tag{8}$$

we arrive at the integral condition

$$\partial_t h + \partial_x q = 0. \tag{9}$$

System (1-7) admits a trivial solution corresponding to a steady constant-thickness film, often called the Nusselt solution (hence the subscript "N" in the following). Assuming $\partial_t \equiv 0$ and $\partial_x \equiv 0$, one simply gets $v \equiv 0$, $p\big|_h = p_a$ and

$$\mu\partial_{yy} u + \rho g \sin\beta = 0,\;\; \partial_y p = -\rho g\cos\beta,\;\; u\big|_0 = 0,\;\; \partial_y u\big|_h = 0,$$

which, for a film of thickness h_N yields:

$$u(y) = \frac{\rho g \sin\beta}{2\mu} y(2h_N - y), \quad p(y) = p_a + \rho g\cos\beta(h_N - y),$$

where the atmospheric pressure p_a is set to zero in the following. The corresponding flow rate is given by

$$q_N = \int_0^h u(y)dy = \frac{\rho g \sin\beta h_N^3}{3\mu},$$

from which an average velocity u_N can be defined by $q_N = h_N u_N$, *i.e.* $u_N = \rho g \sin\beta h_N^2/3\mu$.

At this stage, it is usual to turn to dimensionless equations. Different scalings can be used. The first and most obvious one takes h_N and h_N/u_N as length and time units, see note [26]. Here, we will take another scaling defined without reference to the flow by constructing the length and time units from g (LT^{-2}) and the kinematic viscosity $\nu = \mu/\rho$ (L^2T^{-1}). Taking for convenience $g\sin\beta$ instead of g, this yields $L = \nu^{2/3}(g\sin\beta)^{-1/3}$ and $T = \nu^{1/3}(g\sin\beta)^{-2/3}$. The velocity unit is then $U = LT^{-1} = (\nu g\sin\beta)^{1/3}$. For the pressure, we get $\rho(\nu g\sin\beta)^{2/3}$. The surface tension is then measured by the Kapitza number $\Gamma = \gamma/\left[\rho\nu^{4/3}(g\sin\beta)^{1/3}\right]$. In fact, Kapitza was concerned with vertical planes for which $\beta = \pi/2$ so that the factor $\sin\beta$ did not appear in his definition. It is a matter of convenience to include it or not. The two numbers, with and without, are of the same order of magnitude as long as one does not consider nearly horizontal planes.

Inserting the corresponding variable changes we obtain

$$\partial_t u + u\,\partial_x u + v\,\partial_y u = -\partial_x p + 1 + (\partial_{xx} + \partial_{yy})\,u, \quad (10)$$

$$\partial_t v + u\,\partial_x v + v\,\partial_y v = -\partial_y p - B + (\partial_{xx} + \partial_{yy})\,v, \quad (11)$$

where $B = \cot\beta$ and, for the normal-stress boundary condition at $y = h$

$$\frac{\Gamma\,\partial_{xx} h}{\left[1 + (\partial_x h)^2\right]^{3/2}} + \frac{2}{1 + (\partial_x h)^2}\Big[\partial_x h\Big(\partial_y u\big|_h + \partial_x v\big|_h\Big) - (\partial_x h)^2 \partial_x u\big|_h - \partial_y v\big|_h\Big] + p\big|_h = 0, \quad (12)$$

while the continuity condition (3), the kinematic condition (4) at $y = h$ and the remaining boundary conditions (6,7) are left unchanged. In this unit system where $g\sin\beta = \nu = \rho = 1$, the Nusselt flow rate given by $q_N = u_N h_N = \frac{1}{3}h_N^3$ is numerically equal to the Reynolds number R as defined in note [26].

3 Gradient expansion

Laboratory experiments show that the Nusselt solution may not be relevant, being possibly unstable against waves at the surface of the film. However, as long as the flow rate is not too large, the interface remains smooth at the scale of the film thickness as measured locally by $h(x,t)$. This feature can be introduced as a supplementary assumption and solutions to the equations can be searched in the form of a systematic expansion in powers of a formal parameter ε expressing the smallness of the stream-wise space derivative ∂_x.

At order zero, the problem simply reads

$$\partial_{yy} u^{(0)} = -1, \quad \partial_y p^{(0)} = -B, \quad \partial_y u^{(0)}\big|_h = 0, \quad u^{(0)}\big|_0 = 0, \quad p^{(0)}\big|_h = 0,$$

so that the Nusselt solution is recovered locally with $h(x,t)$ as reference height:

$$u^{(0)}(y) = \frac{1}{2}y(2h - y), \quad v^{(0)} \equiv 0, \quad p^{(0)} = B(h - y), \quad (13)$$

yielding a local flow rate $q^{(0)} = \frac{1}{3}h^3$. This is an exact solution to the problem, provided that the thickness gradient is strictly zero. When this is no longer the case, corrections have to be introduced. Assuming that $h \equiv h(x,t)$ but remains slowly varying, one now looks for a solution "close to" the stationary uniform flow in the form:

$$u = u^{(0)}(h(x,t), y) + u^{(1)}(x,y,t) + u^{(2)}(x,y,t) + \ldots,$$
$$v = v^{(1)}(x,y,t) + v^{(2)}(x,y,t) + \ldots,$$
$$p = p^{(0)}(h(x,t), y) + p^{(1)}(x,y,t) + p^{(2)}(x,y,t) + \ldots,$$

where the corrections are formally of order 1, 2, ...

When developing the calculation systematically, we should notice first that the status of the kinematic interface condition (4) or its integral version (9) is different from that of the other equations. As a matter of fact, the sought-after solution has to be seen as a functional of h and its successive space-time derivatives, all considered as independent quantities. Once it is found at a given order, the result can be inserted in (9) (or (4)), which then presents itself as a constraint relating h and its successive partial derivatives, *i.e.* an evolution equation for h. Furthermore, it is immediately seen that this equation is formally one order higher than the solution found. So, already at zeroth order we get the following nontrivial relation

$$\partial_t h + \partial_x q^{(0)} \equiv \partial_t h + h^2 \partial_x h = 0. \quad (14)$$

However, letting $H = h^2$ leads to $\partial_t H + H\partial_x H = 0$, *i.e.* the Burgers equation, an equation known to produce shocks and hence steep gradients incompatible with the slow-variation assumption. Continuing the expansion is therefore necessary for finding gradient-limiting terms playing the role of viscous dissipation in the Burgers case. Though the result is not guaranteed to be well-behaved, let us review the first steps of the expansion.

At first order we get:

$$\partial_{yy} u^{(1)} - v^{(1)}\partial_y u^{(0)} = \partial_t u^{(0)} + u^{(0)}\partial_x u^{(0)} + \partial_x p^{(0)}, \quad (15)$$

$$\partial_{yy} v^{(1)} - \partial_y p^{(1)} = 0, \quad (16)$$

$$\partial_y v^{(1)} = -\partial_x u^{(0)}, \quad (17)$$

to be solved with the appropriate boundary conditions:

$$p^{(1)}\big|_h - 2\partial_y v^{(1)}\big|_h = 0, \quad (18)$$

$$\partial_y u^{(1)}\big|_h = 0, \quad (19)$$

$$\text{(a)} \quad u^{(1)}\big|_0 = 0, \qquad \text{(b)} \quad v^{(1)}\big|_0 = 0. \quad (20)$$

(Note that $\partial_y u^{(0)}\big|_h = 0$ has been taken into account to simplify the r.h.s. of (18).) Equation (17) yields $v^{(1)} = -\frac{1}{2}y^2\partial_x h$ when making use of (20b). The stream-wise correction $u^{(1)}$ is then obtained from (15) together with boundary conditions (19, 20a) and the pressure correction from (16) subject to (18). We obtain

$$u^{(1)}(x,y,t) = \frac{1}{2}\left(\frac{1}{3}y^3 - h^2 y\right)\partial_t h + \left[\frac{1}{6}\left(\frac{1}{4}y^4 - h^3 y\right)h + B\left(\frac{1}{2}y^2 - hy\right)\right]\partial_x h, \quad (21)$$

$$p^{(1)}(x,y,t) = -(y + h)\partial_x h. \quad (22)$$

To complete the calculation at first order it remains to express the kinematic condition in integral form (9). With $u = u^{(0)} + u^{(1)}$, we obtain for $q = \int_0^h u(y)\,dy$ an expression of the form $\frac{1}{3}h^3 + a(h)\partial_t h + b(h)\partial_x h$, hence the evolution equation for $h(x,t)$:

$$\partial_t h + h^2\partial_x h + \partial_x\left[a(h)\partial_t h + b(h)\partial_x h\right] = 0, \quad (23)$$

where $a(h) = -\frac{5}{24}h^4$ and $b(h) = -\frac{3}{40}h^6 - \frac{1}{3}Bh^3$. The expression of $u^{(1)}$ (21) and equation (23) can be put in simpler forms by noting that the bracketed contribution is already of first order, so that $\partial_t h$ can be replaced by its zeroth order estimate $-h^2\partial_x h$. This leads to:

$$u^{(1)} = \left[\frac{1}{3}\left(\frac{1}{8}y^4 - \frac{1}{2}hy^3 + h^3 y\right)h + B\left(\frac{1}{2}y^2 - hy\right)\right]\partial_x h, \tag{24}$$

$$\partial_t h + h^2\partial_x h + \frac{1}{3}\partial_x\left[\left(\frac{2}{5}h^6 - Bh^3\right)\partial_x h\right] = 0. \tag{25}$$

Looking for a nearly uniform solution $h(x,t) = h_N + \eta(x,t)$ we obtain at lowest order:

$$\partial_t\eta + h_N^2\partial_x\eta + \frac{1}{3}h_N^3\left(\frac{2}{5}h_N^3 - B\right)\partial_{xx}\eta = 0. \tag{26}$$

This shows that in a reference frame moving at velocity $V = h_N^2 = 3u_N$, with coordinate $\xi = x - Vt$, the interface modulations are controlled by a diffusion equation:

$$\partial_t\eta = D\partial_{\xi\xi}\eta, \tag{27}$$

where

$$D = \frac{1}{3}h_N^3\left(B - \frac{2}{5}h_N^3\right), \tag{28}$$

which leads to the known result that fluid films flowing down an inclined plane are unstable against waves ($D < 0$) when their thickness becomes larger than some threshold value h_{Nc} given by: $h_{Nc}^3 = \frac{5}{2}B$ ($= 3R_c$ according to the definition of the Reynolds number R in note [26]). In terms of the flow rate (usual control parameter) we can write $D = \frac{6}{5}q_N(q_{Nc} - q_N)$ where $q_{Nc} = \frac{1}{3}h_{Nc}^3 = \frac{5}{6}B$. Flows along vertical planes are therefore always unstable since $\theta = \pi/2$ implies $B = 0$ and hence $q_{Nc} = 0$, so that $D = -\frac{6}{5}q_N^2 < 0$ for all q_N. Whereas the stabilizing effect of gravity is obvious from the expression of D, the origin of the destabilizing contribution is more difficult to trace back. Instability comes *via* the term $\partial_t u^{(0)}$ in (15) [27] converted into a space derivative term using (14) and partly compensated by the other source terms in (15).

At this stage, gradient-limiting terms playing the role of viscosity for the Burgers equation are effective only for infinitesimal interface fluctuations of thin films at sufficiently low flow rate ($h_N < h_{Nc}$, $q_N < q_{Nc}$, hence $D > 0$). The expansion has therefore to be pushed at higher orders to determine the behavior of thicker films, the more as the amplification rate of the modulations with wave-vector k diverge as $|D|k^2$ for $D < 0$ when k increases. At second order we have

$$\partial_{yy}u^{(2)} - v^{(2)}\partial_y u^{(0)} = \partial_t u^{(1)} + u^{(0)}\partial_x u^{(1)} + u^{(1)}\partial_x u^{(0)} + v^{(1)}\partial_y u^{(1)} - \partial_x p^{(1)} - \partial_{xx}u^{(0)}, \tag{29}$$

$$\partial_{yy}v^{(2)} - \partial_y p^{(2)} = \partial_t v^{(1)} + u^{(0)}\partial_x v^{(1)} + v^{(1)}\partial_y v^{(1)}, \tag{30}$$

$$\partial_y v^{(2)} = -\partial_x u^{(1)}, \tag{31}$$

and

$$p^{(2)}\big|_h - 2\partial_y v^{(2)}\big|_h = -\Gamma\partial_{xx}h, \tag{32}$$

$$\partial_y u^{(2)}\big|_h = 4\partial_x h\partial_x u^{(0)}\big|_h - \partial_x v^{(1)}\big|_h, \tag{33}$$

$$\text{(a)}\quad u^{(2)}\big|_0 = 0, \qquad \text{(b)}\quad v^{(2)}\big|_0 = 0. \tag{34}$$

where (19), (17) and the fact that $\partial_y u^{(0)}\big|_h = 0$ have been used to simplify (32) and (33), respectively. As before, $v^{(2)}$ is derived from (31) subject to (34b), $u^{(2)}$ from (29) using $v^{(2)}$ just found with boundary conditions (33, 34a), which is enough to determine the evolution equation for $h(x,t)$ at this order (see [28] for a detailed computation). In the same time, the pressure $p^{(2)}$ is obtained from (30, 32). So, surface tension effects supposed to smooth out the steep space gradients of interface modulations now enter the solution *via* the boundary condition (32) on $p^{(2)}$. We have thus to continue the expansion and observe that they will enter the solution at third order through a term $-\partial_x p^{(2)}$ in the equation governing $u^{(3)}$ playing the same role as the term $-\partial_x p^{(1)}$ in (29).

It is easy to demonstrate recursively that at each order n the velocity field $u^{(n)}$ can be written in the form of a polynomial in y, h and its derivatives $\partial_x^m h$. A careful examination of the derivation process also shows that, for $n \geq 2$, the term of highest degree in y appearing in $u^{(n)}$ is of degree $4n$ and originates from inertial interactions between the Nusselt flow profile $u^{(0)}$ and its correction at order $n-1$, $u^{(n-1)}$, *via* $u^{(0)}\partial_x u^{(n-1)} + v^{(n)}\partial_y u^{(0)} = u^{(0)}\partial_x u^{(n-1)} - \partial_y u^{(0)}\int_0^y \partial_x u^{(n-1)}\,dy$. Moreover, it can be seen that, if c_n is the coefficient of the term y^{4n} in $u^{(n)}$, then

$$c_{n+1} = -\frac{4n-1}{2(4n+1)(4n+3)(4n+4)}c_n \quad \text{for} \quad n \geq 1,$$

so that $c_2 = -\frac{1}{4480}$, $c_3 = \frac{1}{1520640}$ *etc.*, showing that the contributions of these highest-degree terms become quickly negligible in the evolution equation for h at order n, $\partial_t h + \partial_x(q^{(0)} + \ldots + q^{(n)}) = 0$.

However, the line of thought followed up to now sticks to a strict gradient expansion. Accordingly the different terms retained at a given order in the final evolution equation for h are supposed to scale as the corresponding powers of the gradients ∂_x and ∂_t. As soon as the latter are no longer mathematically infinitesimal, from a physical viewpoint the actual weight of a given term in the solution depends on the conditions of the experiment (Γ, B, q_N). Letting $\mu = \sup_x |h^{-1}\partial_x h|$ measure the space gradient, we observe in particular that the smoothing effects of surface tension scale as $\Gamma\mu^2$ in the expression of the pressure and that, for μ finite but small and Γ large enough, their influence can be felt before that of other terms, even of lower formal order. To make this explicit, we have just to take the term involving Γ into account at a stage of the expansion earlier than that corresponding to its formal order, which can be done already at the lowest possible order, *i.e.* by assuming that the capillary term contributes to the evaluation of the pressure at order zero.

Boundary condition (12) then reads $p\big|_h = -\Gamma\partial_{xx}h$ so that the pressure is no longer given as in (13) but rather by

$$p^{(0)} = B(h-y) - \Gamma\partial_{xx}h. \tag{35}$$

The solution at first order has to be modified accordingly, which yields

$$\partial_t h + h^2\partial_x h + \frac{1}{3}\partial_x\left[\left(\frac{2}{5}h^6 - Bh^3\right)\partial_x h + \Gamma h^3\partial_{x^3}h\right] = 0. \tag{36}$$

instead of (25).

Considering infinitesimal modulations, in lieu of (27) we now get

$$\partial_t\eta = D\partial_{\xi\xi}\eta - K\partial_{\xi\xi\xi\xi}\eta, \tag{37}$$

with $K = \frac{1}{3}h_N^3\Gamma = q_N\Gamma$. As expected from Fourier analysis with perturbations $\propto \exp(ikx)$, the last term in (37) damps out short-wavelength fluctuations, at a rate $-Kk^4$ that dominates the destabilizing contribution $|D|k^2$ when D is negative. The two terms counterbalance each other exactly for a certain cut-off wave-vector k_c given by $k_c^2 = |D|/K = \frac{6}{5}(q_N - q_{Nc})/\Gamma$. This wave-vector defines a scale for which, in order of magnitude, capillary effects enter the problem and work to limit the divergence of space gradients. A low order truncation of the expansion will therefore be acceptable if k_c is physically small enough, which will always be the case close to the instability threshold q_{Nc}.

Equation (36), usually called the Benney equation, is thus expected to govern the interface modulations with space gradients at most of order k_c as long as $k_c \ll 1$, *i.e.* at flow rates close to the threshold in a range depending on the value of Γ. The linear argument above using (37) gives hints on the behavior of solutions to (36) only because the instability turns out to be supercritical, so that a weakly-nonlinear theory accounts for the continuous growth of the amplitude of modulations in the neighborhood of the threshold. In fact, owing to the strong nonlinearities associated with the high powers of h present, this neighborhood is quite narrow and typical solutions to (36) display finite-time singularities not so far from the threshold. From the additive nature of the contribution of the Γ-term in (12) leading directly to (35), it is clear that, depending on the order in ∂_x one decides to introduce it, other gradient terms in h will appear in (36), which will play an effective role if k_c is too large, *i.e.* in general K too small, hence Γ too small. Taking these terms into account does not solve the problem of finite-time singularities, whose origin may be attributed to the strongly nonlinear character of the evolution equation for h, which involves rapidly increasing powers of h as the gradient expansion proceeds.

4 First-order model

In the gradient expansion, the flow variables are supposed to be strictly enslaved to the local thickness h which plays the role of an effective degree of freedom governed by a Benney-like evolution equation. Another approach is then needed to deal with the dynamics of the film in a context where this enslaving is partly relaxed and other effective degrees of freedom are introduced, under the constraint that these new variables should remain slowly variable in x and t and that exact results of the gradient expansion should be recovered in the appropriate limit. Up to now, the hydrodynamic fields (u, v, p) could be expanded on a special set of polynomials in y with slowly varying coefficients functions of $h(x,t)$ and its derivatives. If the flow modulations are sufficiently slow, these fields should not be far from their estimates obtained by the gradient expansion. In other terms, the residue of a Galerkin expansion —or of an approximation derived from a more general weighted residual method— based on these polynomials should be intrinsically small. The coefficients of the expansion would then be considered as the sought-after effective degrees of freedom, and they would be governed by equations generalizing the expressions asymptotically valid when modulations are infinitely slow. The required extension would give some latitude of evolution to these coefficients around the asymptotic value obtained from the gradient expansion. The model developed below is an attempt to implement this general idea in the most "economical" way.

Let us begin with the set of equations consistent at first order except for surface tension effects that, though formally of higher order, are included here owing to their gradient-limiting role, as discussed above. The problem to be solved reads:

$$\partial_t u + u\partial_x u + v\partial_y u + \partial_x p - \partial_{yy}u - 1 = 0, \tag{38}$$

$$\partial_y p + B - \partial_{yy}v = 0, \tag{39}$$

$$\partial_x u + \partial_y v = 0, \tag{40}$$

with boundary conditions

$$p\big|_h + \Gamma\partial_{xx}h - 2\partial_y v\big|_h = 0, \tag{41}$$

$$\partial_y u\big|_h = 0, \tag{42}$$

$$u\big|_0 = 0, \qquad v\big|_0 = 0, \tag{43}$$

and of course the kinematic condition at the interface which, in integral form (9), accounts for mass conservation on average over the thickness.

Integrating (39) with the help of boundary conditions (41–42) we get $p = B(h-y) + \partial_y v + \partial_y v\big|_h - \Gamma\partial_{xx}h$ and further eliminate $\partial_x p$ from (38). Because $\partial_y v = -\partial_x u$ is a first order term, its derivative is of second order and can be dropped of. Therefore, our set of equations read

$$\partial_t u + u\partial_x u + v\partial_y u - \partial_{yy}u = 1 - B\partial_x h + \Gamma\partial_{x^3}h, \tag{44}$$

$$\partial_x u + \partial_y v = 0, \tag{45}$$

with boundary conditions (42–43). (44–45) is sometimes called boundary-layer equations (BL).

Let us now consider the averaging of equation (44) that gives the balance of x-momentum (von Kármán's equation

in the context of boundary layers). We obtain:

$$\int_0^h \left[\partial_t u + u\partial_x u + v\partial_y u - \partial_{yy} u\right] dy = h + \Gamma h \partial_{x^3} h - Bh\partial_x h, \tag{46}$$

which can be transformed into

$$\partial_t \int_0^h u\, dy + \partial_x \int_0^h u^2\, dy = h - \partial_y u\big|_0 + \Gamma h \partial_{x^3} h - Bh\partial_x h. \tag{47}$$

Transformation of the l.h.s. is similar to that leading to (9). The term $\partial_y u\big|_0$, representing the shear at the wall, will be denoted τ_w in the following. On the l.h.s. we recognize $q = \int_0^h u(y)\, dy$ and we can define a new averaged field $r = \int_0^h u^2(y)\, dy$. With these notations (47) reads:

$$\partial_t q + \partial_x r = h\left(1 + \Gamma\partial_{x^3} h - B\partial_x h\right) - \tau_w. \tag{48}$$

Assuming a given velocity profile, one arrives at a set of two equations (9) and (48) for two unknowns h and q, since r can then be computed from q. Simply taking Kapitza's parabolic profile $u(y) \propto \frac{1}{2}\zeta(2-\zeta)$ where $\zeta = y/h$, we have $r = \frac{6}{5}(q^2/h)$, and $\tau_w = 3q/h^2$. Inserting these estimates in (48) we obtain Shkadov's model [22]:

$$\partial_t h = -\partial_x q, \tag{49}$$

$$\partial_t q = h - 3\,\frac{q}{h^2} - \frac{12}{5}\,\frac{q}{h}\,\partial_x q + \left(\frac{6}{5}\frac{q^2}{h^2} - Bh\right)\partial_x h + \Gamma h\partial_{x^3} h. \tag{50}$$

Now, taking (49, 50) as a set of primitive equations, let us consider slow modulations to the uniform solution that verifies $q = \frac{1}{3}h^3 = q^{(0)}$. We are now in position to perform a gradient expansion parallel to the previous one by assuming $q = q^{(0)} + q^{(1)} + q^{(2)} + \ldots$, where $q^{(1)}$, $q^{(2)}$, *etc.* are formally of order 1, 2, *etc.* At lowest order we obtain for the l.h.s. of (50): $\partial_t q^{(0)} = \partial_t(\frac{1}{3}h^3) = h^2\partial_t h = -h^2\partial_x q^{(0)} = -h^2(h^2\partial_x h) = -h^4\partial_x h$, and for the r.h.s.:

$$-3\frac{q^{(1)}}{h^2} + \left[\frac{6}{5}\frac{{q^{(0)}}^2}{h^2} - Bh\right]\partial_x h - \frac{12}{5}\frac{q^{(0)}}{h}\partial_x q^{(0)} + \Gamma h\partial_{x^3} h,$$

where, as before, the surface-tension term has been introduced earlier than dictated by its formal order. This leads to the estimate

$$q^{(1)} = \frac{1}{9}h^6\partial_x h - \frac{1}{3}Bh^3\partial_x h + \frac{1}{3}\Gamma h^3\partial_{x^3} h,$$

which, when replaced in $\partial_t h + \partial_x\left[q^{(0)} + q^{(1)}\right] = 0$, gives the following evolution equation

$$\partial_t h + h^2\partial_x h + \frac{1}{3}\partial_x\left[\left(\frac{1}{3}h^6 - Bh^3\right)\partial_x h + \Gamma h^3\partial_{x^3} h\right] = 0, \tag{51}$$

which differs from equation (36) by the coefficient in front of h^6. This discrepancy leads to an overestimation of the critical Reynolds number $R_{c,IBL} = B$ [29]. Prokopiou *et al.* [8] and Lee and Mei [10] tried to get rid of this discrepancy by starting from systems of equations more complete than (44–45), while keeping the zeroth-order parabolic velocity profile. These approaches failed to recover the correct critical Reynolds number prediction $R_c = \frac{5}{6}B$ and led back to $R_{c,IBL}$. The cause of this failure thus seems to be the lack of flexibility of the assumption about the velocity profile rather than the omission of terms in the set of primitive equations.

In the spirit of Shkadov's assumption, a whole family of models analogous to (49–50), with just different numerical constants, would be obtained by using velocity profiles expressed in terms of a single, possibly better fitted, function of the reduced variable $\zeta = y/h$, $u = a(x,t)\, g(\zeta)$. Such velocity profiles are sometimes called "similar" solutions in boundary-layer theory [30]. The defect of such an approach comes from a somewhat arbitrary freezing of the effective degrees of freedom involved in the velocity field. Here we want to relax part of this constraint by assuming that u is a superposition of functions with slow variable coefficients so that the quantities r and τ_w are less rigidly related to q and h.

So, keeping in mind the results of the long-wavelength expansion, we may reasonably admit that Shkadov's simple assumption, valid at order zero, can be improved by correcting the parabolic profile with the polynomials that appear in the gradient expansion at higher orders, or more precisely, linearly independent combinations of these polynomials adequately chosen for better computational ease. So, let us expand u as

$$u(x,y,t) = b_0(x,t) f^{(0)}(y/h) + b_1(x,t) f^{(1)}(y/h), \tag{52}$$

where $f^{(0)}(\zeta) \equiv -\frac{1}{2}\zeta^2 + \zeta$ and $f^{(1)}(\zeta) \equiv \frac{1}{6}\left(\frac{1}{4}\zeta^4 - \zeta^3 + \zeta^2\right)$. Whereas $u^{(0)}$ in (13) is obviously proportional to $f^{(0)}$, a little algebra is necessary to check that $u^{(1)}$ in (24) can indeed be written as some specific combination of $f^{(0)}$ and $f^{(1)}$ (*cf.* note [31]).

Apart from the fact that the so-far unknown fields b_0 and b_1 are supposed to be slow functions of x and t, by definition of q they must fulfill

$$q = \int_0^h u(y)\, dy = \frac{1}{3}h\left(b_0 + \frac{1}{15}b_1\right). \tag{53}$$

At this stage we have three unknowns, h, b_0, and b_1 but from (53) we see that we can pass to a set formed by h, q and b_1, with b_0 given by $b_0 = (3q/h) - \frac{1}{15}b_1$. Inserting this in $\tau_w \equiv \partial_y u\big|_0 = b_0/h$ we get $\tau_w = (3q/h^2) - (b_1/15h)$. In that way, b_1 appears as a correction to the shear at the plate that would be created by a parabolic velocity profile corresponding to a film with thickness h and flow rate q. To make this explicit, let us re-define b_1 as $b_1 = -15h\tau$ so that

$$\tau_w = \frac{3q}{h^2} + \tau. \tag{54}$$

What we have just done is to pass from the original algebraic variables b_0 and b_1 to the more physically minded variables q and τ. Accordingly (52) can be rewritten as

$$u = \left(\frac{3q}{h} + h\tau\right) f^{(0)}(y/h) - 15h\tau f^{(1)}(y/h). \qquad (55)$$

But, h, q, and τ still make a set of three variables for which we have only two equations (9, 48). Several strategies can be followed to find equations for the unknowns by the method of weighted residual. One can for example average the governing equations with a series of weights. (In the classical Galerkin method the set of weight functions is simply the set of the basis functions, further assumed to fulfill the boundary conditions.) Here equation (48) is just the averaged version of (44) with the trivial uniform weight and, as shown previously, (9) is nothing but the averaged continuity equation (3) simplified by using the kinematic interface evolution equation (4). An alternate method consists in imposing conditions at special points of the domain (collocation). Here, to obtain complementary equations, we will follow this last method and impose the fulfillment of additional conditions at $y = 0$ and $y = h$. These relations will be obtained by differentiating the equations of motion with respect to y and further evaluating them at the boundaries (see [32]). Conditions at $y = 0$ can be interpreted as relations giving the coefficients of a Taylor expansion of the solution as a function of y.

A condition useful at first order is obtained from (44) differentiated with respect to y:

$$\partial_{ty} u + u\partial_{xy} u + v\partial_{yy} u - \partial_{y^3} u = 0,$$

further evaluated at $y = 0$, which gives:

$$\partial_t(\partial_y u\big|_0) - \partial_{y^3} u\big|_0 = 0. \qquad (56)$$

Equation (56) tells us that the fluctuations of the shear at the wall are directly linked to the presence of corrections to the velocity profile beyond the parabolic shape for which they cancel identically. From (55) and (54), further observing that τ is a first-order correction so that the term $\partial_t \tau$ is of higher order and can be dropped from (56), we get the required supplementary equation

$$\partial_t\left(\frac{3q}{h^2}\right) - 15\frac{\tau}{h^2} = 0, \qquad (57)$$

expressing the correction τ in terms of the time derivative of the other fields. Inserting the resulting evaluation of τ_w in (48), using (9) to eliminate $\partial_t h$ and the (here sufficient) zeroth-order estimate $r = \frac{6}{5}(q^2/h)$, we get

$$\partial_t q = \frac{5}{6}h - \frac{5}{2}\frac{q}{h^2} - \frac{7}{3}\frac{q}{h}\partial_x q + \left(\frac{q^2}{h^2} - \frac{5}{6}Bh\right)\partial_x h + \frac{5}{6}\Gamma h\partial_{x^3} h. \qquad (58)$$

When added to (9), equation (58) completes the model at first order as a system of two partial differential equations for the two unknowns h and q. Having the same structure as Shkadov's model but with slightly different coefficients, it will be called "modified Shkadov model". The corrections arise from a better account of the fluctuations of τ_w introduced *via* the third derivative term in (56) by the ζ^3-term in $f^{(1)}$, which can be traced back to the $\partial_t h$ contribution of $u^{(1)}$ in (21) already at the origin of the instability of the plane interface.

Now, let us consider a gradient expansion of (9, 58) similar to the previous ones by assuming $q = q^{(0)} + q^{(1)} + q^{(2)} + \cdots$. We are this time led to

$$q^{(1)} = \frac{2}{15}h^6\partial_x h - \frac{1}{3}Bh^3\partial_x h + \frac{1}{3}\Gamma h^3\partial_{x^3} h,$$

which, when replaced in $\partial_t h + \partial_x\left[q^{(0)} + q^{(1)}\right] = 0$, gives us back the Benney equation (36). So, by construction, the near-critical behavior is correctly predicted by our modified Shkadov model, which no longer overestimates the value of the stability threshold.

Though predictions in the asymptotic domain far beyond the near-critical region are not improved by the correction, a step has clearly been made in the right direction. In particular, the derivation implies that the shear at the wall is a slowly varying quantity. At order zero, q is slaved to h (or the reverse) and τ_w does not fluctuate (injecting a parabolic profile for u in (56) gives $\partial_t(\partial_y u\big|_0) = 0$). At order one, q and h are two independent slowly varying effective degrees of freedom while τ_w remains rigidly linked to q and h through (57). Let us now proceed to the next step. Anticipating the result, we will introduce four additional fields $b_2, \ldots, b_5$ associated with the velocity corrections introduced by the gradient expansion at second order. Supplementary conditions at boundaries analogous to (56) will be derived which, when imposed to the solution will allow us to eliminate these supplementary fields so that we will be left with three equations for three unknowns, h, q and τ, that will play the role of an additional independent effective degree of freedom. The derivation detailed in the next section can be skipped by those only interested in the result, equations (78–80).

5 Second-order model

Let us first write down the set of equations consistent at second order. Clearly all terms in (10), rewritten here for convenience as

$$\partial_t u + u\partial_x u + v\partial_y u + \partial_x p - (\partial_{xx} + \partial_{yy})u - 1 = 0, \qquad (59)$$

are relevant. Such is not the case for (11) which can be simplified as

$$\partial_y p - \partial_{yy} v + B = 0. \qquad (60)$$

It can indeed be seen that the contribution of the terms $\partial_t v + u\partial_x v + v\partial_y v$ is in fact of higher order, owing to the differentiation of p with respect to x in (59) as seen from the calculation leading to (63) below. Of course u and v remain linked by the continuity equation (3).

For the boundary conditions we have

$$p\big|_h + \Gamma\partial_{xx}h - 2\partial_y v\big|_h = 0, \tag{61}$$

$$-4\partial_x h\partial_x u\big|_h + \partial_y u\big|_h + \partial_x v\big|_h = 0, \tag{62}$$

to which we add (43) and of course (9).

Let us transform (59). Integrating (60) with respect to y we get $p(y) = -By + \partial_y v + K$. The integration constant K, in fact a function of x and t, is obtained from (61) which gives $K = Bh + \partial_y v\big|_h - \Gamma\partial_{xx}h$, hence $p = B(h - y) + \partial_y v + \partial_y v\big|_h - \Gamma\partial_{xx}h$. Inserting this expression into (59) we get:

$$\partial_t u + u\partial_x u + v\partial_y u = 1 + \partial_{yy}u - 2\partial_{xy}v + \partial_x\Big[\partial_x u\big|_h\Big] - B\partial_x h + \Gamma\partial_{x^3}h, \tag{63}$$

where the continuity equation has been used to transform $\partial_{xx}u$ into $-\partial_{xy}v$ and $-\partial_y v\big|_h$ into $\partial_x u\big|_h$ (notice that this last term is a function of x and t through h and is differentiated with respect to x as such). Averaging (63) over the thickness h as before we obtain

$$\partial_t q + \partial_x r = h\Big[1 + \Gamma\partial_{x^3}h - B\partial_x h + \partial_x\left(\partial_x u\big|_h\right)\Big] - \tau_w + \partial_y u\big|_h - 2\partial_x v\big|_h,$$

where q, r, and τ_w are defined as before. (The second boundary term $\partial_x v\big|_0$ resulting from the explicit integration of $\partial_{xy}v$ has been dropped since it cancels automatically by virtue of $v\big|_0 \equiv 0$.) Making use of (62) we can simplify this equation: explicitly, we have $h\partial_x\left(\partial_x u\big|_h\right) + \partial_y u\big|_h - 2\partial_x v\big|_h = h\partial_x\left(\partial_x u\big|_h\right) + \left[4\partial_x h\partial_x u\big|_h - \partial_x v\big|_h\right] - 2\partial_x v\big|_h = \left[h\partial_x\left(\partial_x u\big|_h\right) + \partial_x h\partial_x u\big|_h\right] + 3\partial_x h\partial_x u\big|_h - 3\partial_x v\big|_h = \partial_x\left[h\partial_x u\big|_h\right] - 3\partial_x h\partial_y v\big|_h - 3\partial_x v\big|_h = \partial_x\left[h\partial_x u\big|_h\right] - 3\partial_x\left(v\big|_h\right) = \partial_x\left[h\partial_x u\big|_h - 3v\big|_h\right]$. Finally we arrive at

$$\partial_t q + \partial_x r = h\Big[1 + \Gamma\partial_{x^3}h - B\partial_x h\Big] - \tau_w + \partial_x\Big[h\partial_x u\big|_h - 3v\big|_h\Big], \tag{64}$$

to be compared with its first order counter-part (48).

The two first polynomials to be used in addition to $f^{(0)}$ and $f^{(1)}$ are $f^{(2)} = \frac{1}{2}\zeta^2$ and $f^{(3)} = \frac{1}{12}\left(-\frac{1}{2}\zeta^4 + \zeta^2\right)$. The set $\left\{f^{(0)}, f^{(1)}, f^{(2)}, f^{(3)}\right\}$ is easily seen to form a basis of the space of polynomials of degree ≤ 4 that cancel at $y = 0$. The two last polynomials $f^{(4)} = \frac{1}{120}\left(-\frac{1}{6}\zeta^6 + \zeta^5\right)$ and $f^{(5)} = \frac{1}{240}\left(\frac{1}{56}\zeta^8 - \frac{1}{7}\zeta^7 + \frac{1}{3}\zeta^6\right)$ have been chosen so as to permit the reconstruction of all the polynomials entering the gradient expansion at second order. Their seemingly exotic coefficients have been fixed by the additional constraints: $d^5 f^{(4)}/d\zeta^5|_0 = 1$, $d^6 f^{(5)}/d\zeta^6|_0 = 1$, that slightly simplify the forthcoming computations. The velocity component u is expanded as

$$u(x, y, t) = \sum_{k=0}^{5} b_k(x, t) f^{(k)}(y/h),$$

so that, by definition of q, we have

$$q = h\left(\frac{1}{3}b_0 + \frac{1}{45}b_1 + \frac{1}{6}b_2 + \frac{7}{360}b_3 + \frac{1}{840}b_4 + \frac{1}{7560}b_5\right). \tag{65}$$

These new polynomials do not contribute to the evaluation of τ_w which is therefore still given by $\tau_w = b_0/h$.

Sticking to the approach followed for the derivation of the first order model, we keep q and τ as primitive variables in addition to h. In particular τ remains defined from $\tau_w = (3q/h^2) + \tau$, which implies $b_0 = (3q/h) + h\tau$. Inserting this in (65) we obtain $b_1 = -(15h\tau + \frac{15}{2}b_2 - \frac{7}{8}b_3 + \frac{3}{56}b_4 + \frac{1}{168}b_5)$, so that the expression of u extending (55) to second order reads:

$$u = \left(\frac{3q}{h} + h\tau\right) f^{(0)} - \left(15h\tau + \frac{15}{2}b_2 + \frac{7}{8}b_3 + \frac{3}{56}b_4 + \frac{1}{168}b_5\right) \times f^{(1)} + \sum_{k=2}^{5} b_k f^{(k)}, \tag{66}$$

from which $v = -\int_0^y \partial_x u\, dy$ can be derived. To deal with the seven unknowns h, q, τ, b_k, $k = 2, \ldots, 5$, assumed to be slow functions of x and t, we need seven independent equations. In addition to the kinematic condition at the interface (9) and the average x-momentum equation (64) derived earlier, we have the boundary condition (62) on the tangential stress at $y = h$, here used for the first time. To get the remaining four equations we follow the same scheme as for the first-order model and look for collocation at the boundaries.

The equation extending (56) at second order is obtained by differentiating (59) with respect to y, which yields:

$$\partial_{ty}u + u\partial_{xy}u + v\partial_{y^2}u - \partial_{y^3}u - 2\partial_{x^2y}u = 0, \tag{67}$$

where we have used (60) differentiated with respect to x and the continuity equation (3) to eliminate $\partial_{xy}p$. Further evaluating (67) at $y = 0$ gives us

$$\partial_t(\partial_y u\big|_0) - \partial_{y^3}u\big|_0 - 2\partial_{x^2y}u\big|_0 = 0. \tag{68}$$

The evaluation of (67) at $y = h$ leads to an independent equation. The raw condition:

$$\partial_{ty}u\big|_h + u\big|_h\partial_{xy}u\big|_h + v\big|_h\partial_{y^2}u\big|_h - \partial_{y^3}u\big|_h - 2\partial_{x^2y}u\big|_h = 0$$

can be simplified by noting that $\partial_{ty}u\big|_h = \partial_t\left(\partial_y u\big|_h\right) - \partial_{yy}u\big|_h\partial_t h$ and $\partial_{xy}u\big|_h = \partial_x\left(\partial_y u\big|_h\right) - \partial_{yy}u\big|_h\partial_x h$. It is easily checked that the kinematic condition $v\big|_h = \partial_t h + u\big|_h\partial_x h$ at the interface leads to a canceling of terms in $\partial_{yy}u\big|_h$. Furthermore (62) shows that $\partial_y u\big|_h$ is already of second-order so that its x and t derivatives can be neglected. Accordingly, equation (67) evaluated at $y = h$ simply reads

$$\partial_{y^3}u\big|_h + 2\partial_{x^2y}u\big|_h = 0. \tag{69}$$

To obtain simple conditions involving more specifically the variables associated to the high-degree polynomials $f^{(k)}$, $k = 4$, 5, we will add conditions obtained in the same way as (68) but with higher derivatives. The second derivative of (59) brings no new condition on the coefficients of these polynomials since $d^4 f^{(4)}/d\zeta^4$ and $d^4 f^{(5)}/d\zeta^4$ cancel when evaluated at $\zeta = 0$. Thus taking the third derivative of (59), we obtain

$$\partial_t(\partial_{y^3} u\big|_0) + 2\partial_y u\big|_0 \partial_{xy^2} u\big|_0 - \partial_{y^5} u\big|_0 - 2\partial_{x^2y^3} u\big|_0 = 0, \tag{70}$$

and next for the fourth derivative:

$$\partial_t(\partial_{y^4} u\big|_0) + 3\partial_y u\big|_0 \partial_{xy^3} u\big|_0 + 2\partial_{y^2} u\big|_0 \partial_{xy^2} u\big|_0 - 2\partial_{xy} u\big|_0 \partial_{y^3} u\big|_0 - \partial_{y^6} u\big|_0 - 2\partial_{x^2y^4} u\big|_0 = 0. \tag{71}$$

The model at second order is obtained by inserting the ansatz (66) into equations (9,64,62,68–71). In the derivation of the first-order model, the time derivative of τ could be neglected since it was of higher order. This allowed us to eliminate it from the equations to get a system of two equations for the two unknowns h and q. Here this derivative is no longer negligible and τ is a genuine dynamical variable. By contrast, the additional fields are second-order corrections so that their t- or x-derivatives, of still higher order, can be dropped without damage. The derivation, straightforward but (really) tedious, has been performed using MATHEMATICA. Let us consider first the equations accounting for the enslaving of b_2, ..., b_5 to h, q, and τ, namely (62) and (69–71) taken in that order. We obtain

$$\frac{b_2}{h} + \frac{b_4}{30h} + \frac{b_5}{210h} + \frac{3q(\partial_x h)^2}{h^2} - \frac{3\partial_x h\, \partial_x q}{h} + \frac{3q\,\partial_{xx} h}{2h} - \partial_{xx} q = 0, \tag{72}$$

$$-b_3 + \frac{b_4}{3} + \frac{b_5}{15} - \frac{36q(\partial_x h)^2}{h} + 12\partial_x h\, \partial_x q + 6q\,\partial_{xx} h = 0, \tag{73}$$

$$\frac{54q^2\,\partial_x h}{h^6} - \frac{18q\,\partial_x q}{h^5} - \frac{b_4}{h^5} + 15\partial_t\left[\frac{\tau}{h^2}\right] + \frac{54q\,\tau\,\partial_x h}{h^4} - \frac{6\tau\partial_x q}{h^3} - \frac{36q\partial_x \tau}{h^3} = 0, \tag{74}$$

$$9\partial_x\left[\frac{q^2}{h^6}\right] + \frac{b_4 - b_5}{h^6} - 15\partial_t\left[\frac{\tau}{h^3}\right] - \frac{234q\,\tau\,\partial_x h}{h^5} + 9\frac{19q\,\partial_x \tau - 6\tau\,\partial_x q}{h^4} = 0. \tag{75}$$

As already mentioned, partial derivatives of the b_k do not enter these equations so that they can be obtained immediately as functions of h, q, and τ. Indeed b_4 is directly extracted from (74), next b_5 from (75), and finally b_2 and b_3 from (72) and (73), respectively. In fact, the somehow weird definitions of polynomials $f^{(2)}$ to $f^{(5)}$ were intended to make this final evaluation simpler: instead of having the b_k given by the most general (4×4) linear system, we get them by elementary substitution owing to the fact that specific coefficients in this linear system cancel automatically when the corresponding combinations of derivatives are evaluated at $y = 0$ or $y = h$.

To terminate the derivation of the second-order model, it remains to substitute the expressions of the b_k in the dynamical equations for h, q and τ, that is to say the kinematic condition at the interface (9), the average x-momentum balance equation (64) that now reads

$$\partial_t q + \partial_x\left[\frac{6q^2}{5h} - \frac{2}{35}hq\tau\right] = -\frac{3q}{h^2} - \tau + h + \partial_x\left[\frac{9\partial_x q}{2} - \frac{6q\partial_x h}{h}\right] - Bh\partial_x h + \Gamma h\partial_{x^3} h, \tag{76}$$

and the stress balance at $y = 0$:

$$-\frac{15\tau}{h^2} + \partial_t\left[\frac{3q}{h^2}\right] + \partial_t\tau - \partial_{xx}\left[\frac{6q}{h^2}\right] - \frac{1}{h^3}\left[\frac{15}{2}b_2 + \frac{7}{8}b_3 + \frac{3}{56}b_4 + \frac{1}{168}b_5\right] = 0. \tag{77}$$

At last we obtain

$$\partial_t h = -\partial_x q, \tag{78}$$

$$\partial_t q = h - \frac{3q}{h^2} - \tau + \partial_x\left[\frac{2}{35}h\tau q - \frac{6q^2}{5h} - \frac{6q\partial_x h}{h} + \frac{9\partial_x q}{2}\right] - Bh\partial_x h + \Gamma h\partial_{x^3} h, \tag{79}$$

$$\partial_t \tau = \frac{7}{h} - \frac{21q}{h^4} - \frac{42\tau}{h^2} - \frac{18q^2\partial_x h}{5h^4} + \frac{6q\partial_x q}{5h^3} + \frac{2q\tau\partial_x h}{5h^2} + \frac{\tau\partial_x q}{15h} - \frac{3q\partial_x \tau}{5h} + \frac{84q(\partial_x h)^2}{h^4} - \frac{63\partial_x q\partial_x h}{h^3} - \frac{7B\partial_x h}{h} + \frac{7\Gamma\partial_{x^3} h}{h}. \tag{80}$$

A gradient expansion up to second order assuming $q = q^{(0)} + q^{(1)} + q^{(2)}$ and $\tau = \tau^{(1)} + \tau^{(2)}$ leads to

$$q^{(2)} = \left(\frac{7}{3}h^3 - \frac{8}{15}B\,h^6 + \frac{127}{315}h^9\right)(\partial_x h)^2 + \left(h^4 - \frac{10}{63}B\,h^7 + \frac{4}{63}h^{10}\right)\partial_{x^2} h,$$

$$\tau^{(2)} = \left(2h - \frac{4}{15}B\,h^4 + \frac{13}{63}h^7\right)(\partial_x h)^2 + \left(\frac{1}{2}h^2 - \frac{8}{105}B\,h^5 + \frac{2}{63}h^8\right)\partial_{x^2} h,$$

yielding the exact second-order evolution equation [6] as expected.

At this stage, one can notice that the second-order formulation includes the effects of the stream-wise dissipation, while they are absent from the first-order model,

and more generally from any expansion based on the first-order BL equations (44, 45). As a matter of fact, performing the same derivation at second order with this system, one obtains

$$\partial_t h = -\partial_x q, \tag{81}$$

$$\partial_t q = h - \frac{3q}{h^2} - \tau + \partial_x\left[\frac{2}{35}h\tau q - \frac{6q^2}{5h}\right] - Bh\partial_x h + \Gamma h\partial_{x^3} h, \tag{82}$$

$$\partial_t \tau = \frac{7}{h} - \frac{21q}{h^4} - \frac{42\tau}{h^2} - \frac{18q^2\partial_x h}{5h^4} + \frac{6q\partial_x q}{5h^3} + \frac{2q\tau\partial_x h}{5h^2} + \frac{\tau\partial_x q}{15h} - \frac{3q\partial_x \tau}{5h} - \frac{7B\partial_x h}{h} + \frac{7\Gamma\partial_{x^3} h}{h}, \tag{83}$$

where it can be seen that terms of the form $\partial_{xx}()$ or $\partial_x()\partial_x()$, are absent. By difference with (78–80), such terms have thus to be attributed to the effects of streamwise viscous dissipation.

6 Linear stability analysis

Before presenting our preliminary numerical results with the model equations developed in Sections 4 and 5, let us compare their linear stability properties with the data collected by Liu *et al.* [33]. Setting $w = w_N + \bar{w}\exp[i(kx - \omega t)]$ where w and w_N refer to h and q and their values for the reference Nusselt flow solution, linearizing (9, 58), we obtain

$$\omega\,\bar{h} = k\,\bar{q},$$

$$\left(\frac{5}{2} + i\left(\frac{1}{9}h_N^4 - \frac{5}{6}Bh_N\right)k - i\frac{5}{6}\Gamma h_N k^3\right)\bar{h} = \left(\frac{5}{6} + i\frac{7}{27}h_N^4 k - i\frac{1}{3}h_N^2\omega\right)\bar{q}.$$

Compatibility of this system yields the dispersion relation. For easier comparison with experimental results, it is preferable to turn to a scaling where h_N is the length scale. This leads to change k into k/h_N, ω into ωh_N, and to introduce the Reynolds and Weber numbers, $R = \frac{1}{3}h_N^3$ and $W = \Gamma/h_N^2$ respectively.

$$k + i\left(\frac{2}{15}R - \frac{1}{3}B\right)k^2 - i\frac{1}{3}Wk^4 + \left(-1 - i\frac{14}{15}Rk\right)\omega + i\frac{6}{5}R\omega^2 = 0. \tag{84}$$

Separating real and imaginary parts for real k and ω we get

$$\omega = k, \tag{85}$$

$$\frac{6}{5}R - B = Wk^2. \tag{86}$$

Equation (86) defines the neutral stability curve of the modified Shkadov model in the plane (R, k) while (85) implies that the phase speed $c = \omega/k$ is constant and equal to unity at marginality. As expected, equations (85–86) characterize the marginal waves of Benney's equation (36) [13] (For comparison, linear stability analysis of Shkadov's model (49–50) would lead to $R - B = Wk^2$.).

Following Yih [34], let us consider the temporal stability problem in terms of an asymptotic expansion of frequency ω in powers of a real wave-number k in the limit $k \ll 1$. We get

$$\omega = k + i\,k^2\left(\frac{2}{5}R - \frac{1}{3}B\right) + k^3\left(\frac{22}{45}BR - \frac{44}{75}R^2\right) + i\,k^4\left(-\frac{2}{15}B^2R + \frac{28}{27}BR^2 - \frac{1184}{1125}R^3 - \frac{1}{3}W\right) + \mathcal{O}(k^5), \tag{87}$$

to be compared with the exact asymptotic expansion of Orr–Sommerfeld equation,

$$\omega = k + i\,k^2\left(\frac{2}{5}R - \frac{1}{3}B\right) + k^3\left(-1 + \frac{10}{21}BR - \frac{4}{7}R^2\right) + i\,k^4\left(\frac{3}{5}B - \frac{471}{224}R - \frac{2}{15}B^2R + \frac{17363}{17325}BR^2 - \frac{75872}{75075}R^3 - \frac{1}{3}W\right) + \mathcal{O}(k^5). \tag{88}$$

Although equation (87) is close to (88), three terms are missing in (87). A careful examination of the calculus shows that these terms mostly originate from second-order viscous terms omitted in the derivation of (9–58).

A parallel stability analysis of the second-order model (78–80) leads to the dispersion relation

$$\mathsf{A}(k) + \mathsf{B}(k)\omega + \mathsf{C}(k)\omega^2 + \mathsf{D}(k)\omega^3 = 0, \tag{89}$$

with

$$\mathsf{A}(k) = k + i\left(\frac{1}{5}R - \frac{1}{3}B\right)k^2 + \left(\frac{4}{5} - \frac{2}{1225}R^2 + \frac{1}{105}BR\right)k^3 + i\left(\frac{2}{175}R - \frac{1}{3}W\right)k^4 + \frac{1}{315}Wk^5,$$

$$\mathsf{B}(k) = -1 - i\frac{38}{35}Rk + \left(-\frac{9}{5} + \frac{6}{245}R^2 - \frac{1}{35}BR\right)k^2 - i\frac{29}{350}Rk^3 - \frac{3}{105}WRk^4,$$

$$\mathsf{C}(k) = i\frac{9}{7}R - \frac{3}{35}R^2k + i\frac{9}{70}Rk^2, \mathsf{D}(k) = \frac{3}{35}R^2.$$

The asymptotic expansion of (89) in the temporal domain ($k \in \mathbb{R}$) gives

$$\omega = k + i\,k^2\left(\frac{2}{5}R - \frac{1}{3}B\right) + k^3\left(-1 + \frac{10}{21}BR - \frac{4}{7}R^2\right) + i\,k^4\left(\frac{3}{5}B - \frac{376}{175}R - \frac{2}{15}B^2R + \frac{3683}{3675}BR^2 - \frac{1238}{1225}R^3 - \frac{1}{3}W\right) + \mathcal{O}(k^5), \tag{90}$$

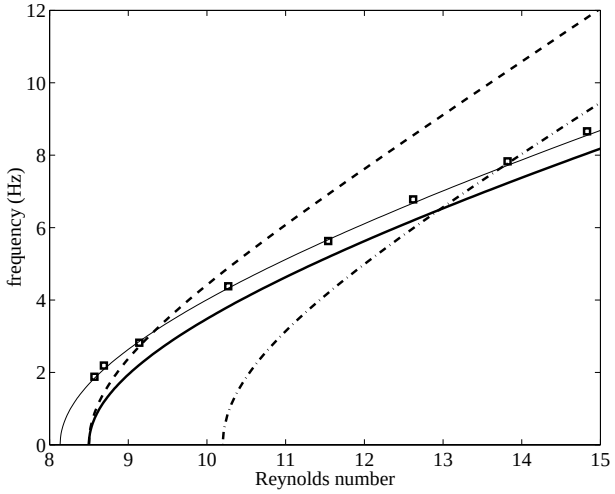

Fig. 2. Neutral stability curve for glycerin-water films at $\beta = 5.6°$ and $\Gamma = 700.15$. The cut-off frequency is shown as a function of the Reynolds number. The thick solid line is the prediction of the second-order model, the thin one is a fit with experimental data of Liu and Gollub [33] displayed as squares. See text for dashed and dot-dashed lines that correspond to the first-order and Shkadov's model respectively.

which is now very close to (88). All terms are present to the considered order in k and coefficients differ by no more than 3% from the exact result. The remaining discrepancy between (90) and the exact asymptotic result can be attributed to the omission of the inertial terms $\partial_t v + u\partial_x v + v\partial_y v$ in the y-momentum equation (11) owing to the fact mentioned earlier that monomials of higher degree involved in the velocity profile contribute very little to the coefficients of the gradient expansion at third order.

The neutral stability curve of (89), the spatial growth rate $-\mathcal{I}m(k)$ and phase speed $\mathcal{R}e(\omega/k)$ have been determined for a set of parameters corresponding to the experiments of Liu *et al.* [33] using a standard predictor-corrector Euler–Newton continuation scheme [35]. Figure 2 shows excellent agreement between our second-order model (thick solid line) and the experimental data (squares) for the cut-off frequency. Predictions from Shkadov's model and from our modified first-order model (9–58) are also displayed as dot-dashed and dashed lines, respectively. It is clear from the figure that the latter predicts the threshold correctly, while the former overestimates it somehow. The increasing discrepancy between the first-order and the second-order predictions must be attributed to the neglect of stream-wise viscous dissipation. As a matter of fact, starting with the BL equations (44–45) that also neglects this contribution, one is led to (81–83) at second-order. A dispersion relation with the same structure as (89) but with missing terms corresponding to it can be derived (see note [36]), and it can be checked that marginal properties are still given by (85–86), which translates into the dashed line in Figure 2. A similar improvement was obtained by Yu *et al.* [9] who developed a linear stability analysis of BL equations at second-order including both a heuristic term accounting for pressure variation across the film and viscous stream-wise dissipation, even at large Reynolds number. The slight discrepancy between experiments and our theory remains unexplained but we can remark that it is closely comparable to that already reported in [33]. As a matter of fact, improved agreement (light solid line in Fig. 2) can easily be obtained by adjusting the value of the theoretical threshold to that extrapolated from experimental data, which can be done by changing the slope from $\beta = 5.6°$ to $5.85°$, or by adopting a slightly different set of physical constants for the fluid mixture.

Spatial linear stability properties ($\omega \in \mathbb{R}$, $k \in \mathbb{C}$) for equations (84) and (89) with or without second-order viscous terms, are compared with experimental results in Figure 3. For the phase speed (Fig. 3b), predictions of the various approximations are very close to each other and discrepancies with experimental data (squares) are not significant. By contrast, for the growth-rate (Fig. 3a) the agreement is again excellent for the full second-order model (solid line). With respect to predictions of the first-order —dashed— and simplified second-order model (81–83) —dot-dashed— it can be seen that the curves remain close to each other. As a consequence of the degeneracy of the marginal problem mentioned above, they intersect precisely at zero growth-rate and phase-speed equal to unity. On the contrary, the full second-order model predicts a significantly lower growth-rate so that the marginal condition is obtained for a smaller phase-speed, which explains the discrepancy illustrated in Figure 2.

7 Spatial evolution of nonlinear periodic waves

Comparison of fully nonlinear solutions to our second-model (78–80) with experiments performed by Liu and Gollub [4] has been attempted by numerical simulations corresponding to a periodic upstream forcing. A second-order finite-difference quasi-linearized Crank-Nicholson scheme [37] has been implemented to deal with the high-order nonlinearities involved. Owing to the convective character of the instability that sweeps disturbances continuously away from the computational domain, the boundary condition at the downstream end could be treated in a non-physical way by truncating the discretized equations at the relevant nodes. The scheme was seen to be satisfactory in that inaccuracies remained confined to a very small downstream numerical boundary layer and never invaded the upstream region. The upstream boundary condition was chosen as a periodically forced flow rate

$$q(0,t) = q_N(1 + A\cos\omega t)$$

to fit with Liu and Gollub's flow-rate control *via* the entrance pressure manifold. The length of the wave inception region depends on the forcing amplitude. The conversion of the relevant physical quantity into a numerical parameter being out of reach, we have chosen to compare the

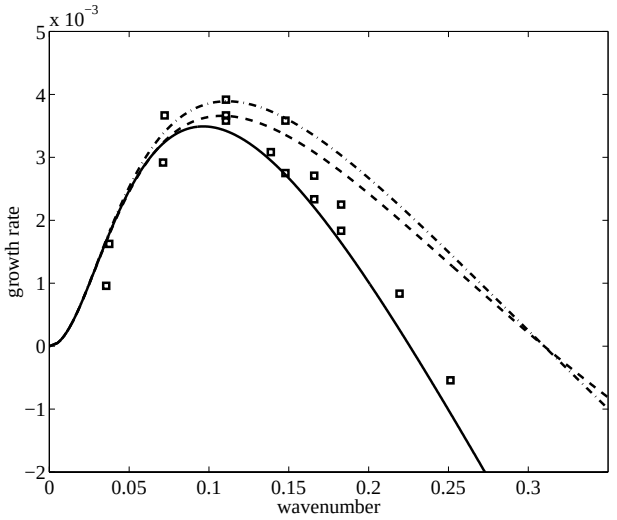

Fig. 3. Dispersion of linear waves for glycerin-water films with $\beta = 4.6°$, $R = 15.33$ and $\Gamma = 797.2$ corresponding to the experiments of Liu and Gollub (squares) and predictions of various models. (a) Spatial growth rate. (b) Phase velocity. The solid lines derive from the dispersion relation of the second-order model. Dashed lines and dot-dashed lines corresponds to the first-order model and the second-order model with stream-wise second-order dissipation terms omitted.

waves at corresponding amplitude levels without trying to adjust the distance to the origin of the flow, in other terms the abscissa frame is given up to some unknown translation. We first present results corresponding to a multi-peaked wave regime in Figure 4. The form and amplitude of the numerical wave profiles are in striking agreement with the experiment. In particular, the small depression appearing on the primary peak, passing the primary front and then locking its phase to form a subsidiary peak of the wave-front is evident both in the simulation and in the experiment. The modulation of the experimental wave-train further downstream is also well captured by the simulation. Figure 5 compares laboratory and computer results for a low-frequency forcing ending in near-solitary stationary wave-trains. The comparison is again very good, though our numerics predict amplitudes somewhat larger than in the experiment. The capillary ripples downstream the main hump are also slightly more pronounced and the wavelength of the stationary train a little smaller. The use of phase-sensitive averaging technique that might have smoothed the steepest parts of the experimental wave profiles could partly explain the larger discrepancies observed in Figure 5 when compared to Figure 4. Our results are also in good agreement with direct numerical simulations performed by Ramaswamy *et al.* (see Figs. 15 and 17 of [19]) who also report larger amplitudes of the fronts.

We have also compared our numerical results to experimental ones of Alekseenko *et al.* [38]. Though their geometry was cylindrical, the thickness-to-diameter ratio was sufficiently large for curvature effects to be negligible. Figure 6 displays the profile and streamlines of a stationary large-amplitude near-solitary wave for parameters in Figures 5, 6, and Table 1 of [38]. Streamlines show evidence of a large recirculation region inside the hump. Such recirculations have been inferred from experimental wave profiles by numerical reconstruction using the NS equations [41] and were already present in solutions to the BL equations [21].

Alekseenko *et al.* measured the mean film thickness $\langle h \rangle$, the peak height h_{max}, the wavelength λ, the speed c of the waves, and the mean surface velocity $\langle U \rangle$. Comparison with our data is given in Table 1. Though the speed and wavelength were provided with the experimental data, the forcing frequency (the genuine control parameter) was not given. The uncertainty about its value may partly explain the differences between experimental and numerical values. At any rate, it is remarkable that the mean film thickness $\langle h \rangle$ is much smaller than the Nusselt film thickness $h_N = 0.582$ mm for both the experiment and the simulation. The wave profile in Figure 6 is strikingly similar to the sketches in [38]. By contrast, solutions of Shkadov's model by Tsvelodub and Trifonov [24] (*cf.* Fig. 15 of [24]a) and of BL equations by Chang *et al.* [39,40] exhibit a large number of capillary ripples in front of the main hump. This feature can probably be attributed to the lack of dispersion associated to the second-order stream-wise viscous dissipation terms omitted in BL equations.

8 Conclusion

From a theoretical point of view, the dynamics of film flows down inclined planes can be studied at different approximation levels, ranging from direct simulations of the full NS equations to the simple KS equation. While the latter gives an over-simplified picture of the problem, appropriate for near-infinitesimal thickness modulations of the flat film basic flow at the limit of strong interfacial effects, the former turn out to be untractable in any realistic 3-dimensional situation, hence the need of modeling at some intermediate level. Fortunately enough,

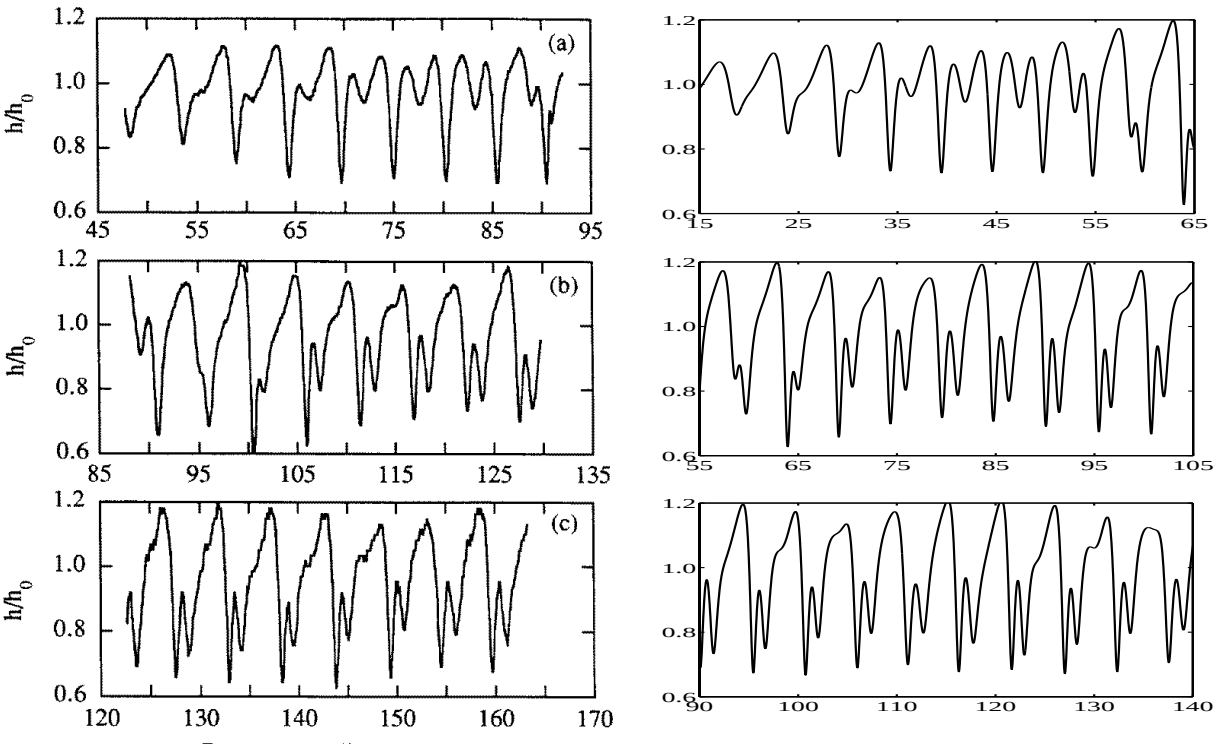

Fig. 4. Comparison between experiments (left) and simulation (right). The plane is inclined to 6.4° from horizontal, liquid is glycerin-water and Reynolds number $R = 19.33$ [4]. The figure shows three snapshots of the film thickness at three different locations on the plane from upstream (top) to downstream (bottom) at forcing frequency 4.5 Hz. Units are identical in the experiment and the simulation (here $h_0 \equiv h_N$).

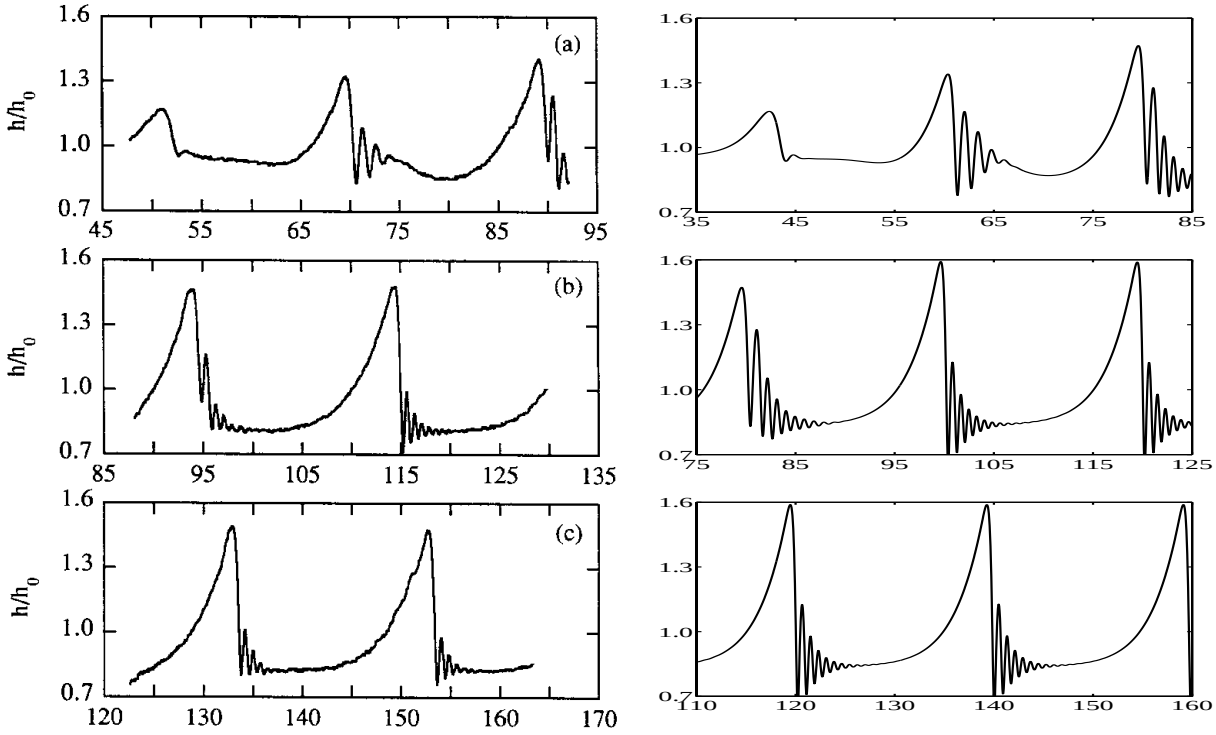

Fig. 5. Comparison between experiment (left) and simulation (right) for low-frequency forcing at 1.5 Hz. Parameters are identical to those in Figure 4.

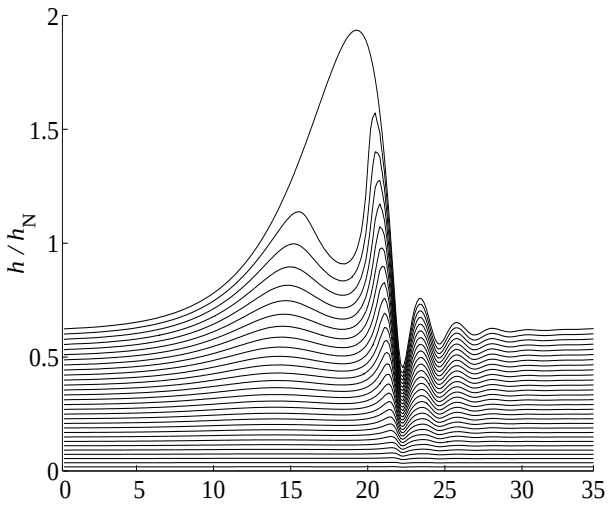

Fig. 6. Simulation of a periodically forced vertical film at $f = 2.034$ Hz, $\nu = 7.2\,10^{-6}\,\mathrm{m}^2/\mathrm{s}$ and $\gamma/\rho = 57.6\,10^{-6}\,\mathrm{m}^3/\mathrm{s}^2$ (*i.e.* $R = 12.4$ and $\Gamma = 193.6$) corresponding to the data of Alekseenko, *et al.* [38] and leading to the formation of a near-solitary stationary wave-train. Streamlines are plotted in a reference frame moving at the speed of the wave. Notice the large recirculation region in the hump. Wave characteristics are listed in Table 1.

at sufficiently low Reynolds numbers instabilities develop at long wavelengths, which legitimates approaches resting on truncated gradient expansions. The resulting simplification of NS equations yields so-called boundary layer equations that are slightly simpler to solve but remain partial differential equations of maximal space dimension (3 or 2 according to whether one considers transverse perturbations or not). They remain valid up to a point where the assumption about the thickness modulations become untenable, which depends on the strength of interfacial effects but is usually believed to happen above $R \sim 300$ [1]. The next reduction step is taken by eliminating irrelevant velocity degrees of freedom. Complete elimination of the velocity field ends in Benney-like equations only involving the local film thickness h and its gradients. They are asymptotically valid but, unfortunately, the lowest significant truncation, namely the Benney equation itself, already displays finite time singularities beyond some critical (and rather low) Reynolds number where one-hump solitary solutions disappear [13]. Less drastic approximations have to keep some trace of flow variables in addition to h. Within the truncated gradient expansion, the velocity field is then projected on a (small) set of functions. Equations governing the corresponding amplitudes are searched for by weighted residual methods, with the goal of obtaining realistic evolutions free of non-physical singularities. Such models should have thus essentially the same range of validity as BL equations but now no longer involve fields depending on the cross-flow coordinate y but amplitudes that depend only on the stream-wise x and transverse z coordinates, *i.e.*, one space-dimension less, which makes them much easier to analyze or simulate. The simplest such model due to Shkadov [22] just involves h and the local flow rate $q = \int_0^h u(y)\,dy$ and is obtained by assuming a parabolic flow profile and averaging the BL equations at lowest order over the film thickness. Though it yields qualitatively good results in the nonlinear regime, it fails to predict the critical behavior quantitatively. In order to overcome its limitations we have developed a more sophisticated approach that also rests on averaged equations but deals with a more flexible velocity profile based on the polynomials appearing in Benney's expansion. Among various weighted residual strategies, we have chosen a method of collocation at boundaries. The resulting additional conditions are identities that have to be fulfilled by the solutions, which determine relations between unknown coefficients in the expansion of the velocity field, further understood as successive terms (obtained by identification) of a Taylor series approximation to this field. We have developed several other variants of the method of weighted residuals, obtaining models with similar structure. The interest of the present strategy lies in the fact that the gradient expansion of the model matches exact results asymptotically. Linear stability analysis has shown that second-order modeling correctly predicts the threshold, the spatial phase-speed and growth-rate beyond criticality in the range of parameters corresponding to laboratory experiments. Subsequent numerical simulation of the spatial evolution of forced films did not show finite-time blow-up often encountered with Benney-like equations for which all variables except the film-thickness h are adiabatically eliminated. Good quantitative agreement with both numerical and experimental results was obtained even for large amplitude waves without adjustable parameters. Proper account of the streamwise viscous dissipation was seen to be crucial for the improvement of the theoretical predictions.

In the spirit of dynamical systems theory, a study of the families of stationary wave solutions to the first and second-order models has been undertaken, also showing good agreement with the direct numerical simulations of Salamon *et al.* [18]. In particular, we were able to recover their bifurcation diagram showing a cusp catastrophe at a quantitative level (see [42] for a preliminary report).

All these results thus strongly encourage us not only to perform a detailed investigation in the parameters space R, B and Γ in the case of two-dimensional film-flow but to turn bravely to the three-dimensional case. The strategy has been to describe the structure of the flow in terms of a small number of fields with clear physical significance, the film thickness h, the instantaneous flow rate q and the variable τ measuring the departure of the wall shear stress from the parabolic profile prediction. These quantities serve to reconstruct the full flow field. This approach, which comes to replace the dependence on the normal coordinate y by a small set of variables, can be extended straightforwardly to three dimensions. The corresponding reduction will lead to few partial differential evolution equations in x and z. Besides being much less demanding of numerical resources for their simulation,

Table 1. Wave characteristics corresponding to Figure 6. Top line: Experimental observations. Bottom line: Numerical results.

$\langle h \rangle$ mm	h_{max} mm	λ mm	c mm/s	c $q_N/\langle h \rangle$	$\langle U \rangle$ $q_N/\langle h \rangle$
0.545	1.12	36	460	2.83	1.27
0.514	1.13	34	434	3.20	1.30

the study of these equations should give clearer insight in the physical mechanisms at the origin of secondary three-dimensional instabilities observed in experiments [3].

The modeling of film flows over inclined planes thus offers to us a unique opportunity of understanding the transition to turbulence *via* spatio-temporal chaos in open-flow configurations, hinting at other hydrodynamic problems such as boundary-layer stability.

This work was supported by a grant from the Délégation Générale à l'Armement (DGA) of the French Ministry of Defense. The authors would like to thank J.M. Chomaz, B.S. Tilley and I. Delbende for stimulating discussions. Thanks are warmly extended to T. Lescuyer, J. Webert and C. Cossu for their kind and helpful assistance.

References

1. H.C. Chang, Annu. Rev. Fluid Mech. **26**, 103–136 (1994).
2. J.M. Floryan, S.H. Davis, R.E. Kelly, Phys. Fluids **30**, 983–989 (1987).
3. J. Liu, B. Schneider, J.P. Gollub, Phys. Fluids **7**, 55–67 (1995).
4. J. Liu, J.P. Gollub, Phys. Fluids **6**, 1702–1712 (1994).
5. J. Benney, J. Math. Phys. **45**, 150–155 (1966).
6. S.P. Lin, J. Fluid Mech. **63**, 417–429 (1974).
7. P.L. Kapitza, S.P. Kapitza, Zh. Ekper. Teor. Fiz. **19**, 105 (1949); Also in *Collected papers of P.L. Kapitza*, edited by D. Ter Haar, pp. 690–709.
8. T. Prokopiou, M. Cheng, H.C. Chang, J. Fluid Mech. **222**, 665–691 (1991).
9. L.-Q. Yu, F.K. Wasden, A.E. Dukler, V. Balakotaiah, Phys. Fluids **7**, 1886–1902 (1995).
10. J.-J. Lee, C.C. Mei, J. Fluid Mech. **307**, 191–229 (1996).
11. E.A. Demekhin, M.A. Kaplan, V.Y. Shkadov, Izv. Ak. Nauk SSSR, Mekh. Zhi. Gaza **6**, 73–81 (1987).
12. Actually, considering only small surface tension effects, Benney never expressed any truncation of his expansion in the form (36). To our knowledge, the first occurrence of (36) is in: B. Gjevik, Phys. Fluids **13**, 1918–25 (1970).
13. A. Pumir, P. Manneville, Y. Pomeau, J. Fluid Mech. **135**, 27–50 (1983).
14. Y. Kuramoto, T. Tsuzuki, Prog. Theor. Phys. **55**, 536 (1976); G.I. Sivashinsky, Acta Astronautica **4**, 356 (1977); Y. Kuramoto, Prog. Theor. Phys. Suppl. **64**, 1177 (1978).
15. O.Y. Tsvelodub, Izv. Ak. Nauk SSR, Mekh. Zh. Gaza **4**, 142–146 (1980).
16. H.C. Chang, Phys. Fluids **29**, 3142–3147 (1986).
17. S.W. Joo, S.H. Davis, S.G. Bankoff, Phys. Fluids. A **3**, 231–232 (1991).
18. T.R. Salamon, R.C. Armstrong, R.A. Brown, Phys. Fluids **6**, 2202–2220 (1994).
19. B. Ramaswamy, S. Chippada, S.W. Joo, J. Fluid Mech. **325**, 163–194 (1996).
20. E.A. Demekhin, I.A. Demekhin, V.Y. Shkadov, Izv. Ak. Nauk SSSR, Mekh. Zhi. Gaza **4**, 9–16 (1983).
21. H.C. Chang, E.A. Demekhin, D.I. Kopelevitch, J. Fluid Mech. **250**, 433–480 (1993).
22. V.Y. Shkadov, Izv. Ak. Nauk SSSR, Mekh. Zhi. Gaza **2**, 43–51 (1967).
23. B.A. Finlayson, *The method of weighted residuals and variational principles, with application in fluid mechanics, heat and mass transfer* (Academic Press, 1972).
24. (a) Y.Y. Trifonov, O.Y. Tsvelodub, J. Fluid Mech. **229**, 531–554 (1991); (b) O.Y. Tsvelodub, Y.Y. Trifonov, J. Fluid Mech. **244**, 149–169 (1992).
25. H.C. Chang, E.A. Demekhin, D.I. Kopelevitch, Physica D **63**, 299–320 (1993).
26. The relative importance of inertia and viscous effects is then characterized by the Reynolds number $R = \rho u_N h_N/\mu$, whereas surface tension γ is measured by the Weber number $W = \gamma/(\rho g \sin\beta h_N^2)$ *via* the stream-wise component of the gravitational acceleration $g \sin\beta$.
27. M.K. Smith, J. Fluid Mech. **217**, 469–485 (1990).
28. C. Nakaya, Phys. Fluids **18**, 1407–1412 (1975).
29. M. Cheng, H.C. Chang, Phys. Fluids **7**, 34–54 (1995).
30. H. Schlichting, *Boundary-layer theory* (McGraw-Hill, 1955).
31. Polynomial $f^{(1)}$ is chosen such that $df^{(1)}/d\zeta|_0 = 0$, $d^3 f^{(1)}/d\zeta^3|_0 = -1$. This choice is in line with those made for the higher degree polynomials used later, which are in turn justified by the fact that we use collocation residuals at the boundary points $\zeta = 0$ and $\zeta = 1$.
32. J. Villadsen, M.L. Michelsen, *Solution of differential equation models by polynomial approximation* (Prentice-Hall, 1978).
33. J. Liu, J.D. Paul, J.P. Gollub, J. Fluid Mech. **250**, 69–101 (1993).
34. C.S Yih, Phys. Fluids **6**, 321–334 (1963).
35. E.L. Allgower, K. Georg, *Numerical continuation methods* (Springer-Verlag, 1990).
36. Namely, $\frac{4}{5}k^3 + i\frac{2}{175}Rk^4$ in $\mathsf{A}(k)$, $-\frac{9}{5}k^2 - i\frac{29}{350}Rk^3$ in $\mathsf{B}(k)$, and $i\frac{9}{70}Rk^2$ in $\mathsf{C}(k)$.
37. R.D. Richtmeyer, K.W. Morton, *Difference methods for initial value problems* (Interscience, 1967).
38. S.V Alekseenko, V.Y. Nakoryakov, B.G. Pokusaev, AIChE J. **31**, 1446–1460 (1985).
39. H.C. Chang, E.A. Demekhin, E. Kalaidin, J. Fluid Mech. **294**, 123–154 (1995); AIChE J. **42**, 1553–1568 (1996).
40. Demekhin *et al.* have shown that the set of control parameters can be reduced to a single reduced Reynolds number δ for the BL equations and a vertical plane [20]. The solitary wave in Figure 6 corresponds to $\delta = 0.056$ and speed $c = 7.33\,u_N$, to be compared with results in [39].
41. F.K. Wasden, A.E. Duckler, AIChE J. **35**, 187–195 (1989).
42. C. Ruyer-Quil, P. Manneville, *Transition to turbulence of fluid flowing down an inclined plane: Modeling and simulation*, *Proceedings of the 7th European Turbulence Conference*, Saint Jean Cap Ferrat, June 30-July 3, 1998, in *Advances in Turbulence VII*, edited by U. Frisch, (Kluwer, 1998), pp. 93-96.